16èmes Journées de l'Hydrodynamique
27-29 novembre 2018 - Marseille
CENTRALE MARSEILLE
irphé Institut de Recherche sur les Phénomènes Hors Equilibre

ÉTUDE EXPÉRIMENTALE DU SILLAGE DERRIÈRE DE LARGES OBSTACLES POSÉS SUR LE SOL

EXPERIMENTAL ANALYSIS OF THE WAKE PAST WIDE WALL-MOUNTED OBSTACLES

Maria IKHENNICHEU[(1)], Grégory GERMAIN[(1)], Philippe DRUAULT[(2)], Benoît GAURIER[(1)]

maria.ikhennicheu@ifremer.fr ; gregory.germain@ifremer.fr ; philippe.druault@upmc.fr
benoit.gaurier@ifremer.fr

[(1)]Ifremer, Marine Structure Laboratory, 150 Quai Gambetta 62200 Boulogne sur Mer, France.
[(2)]Sorbonne Université, UPMC Univ Paris 06, CNRS, UMR 7190, Institut Jean Le Rond d'Alembert, F-75005 Paris, France

Résumé

Dans les zones à forts courants telles que celles adaptées à l'exploitation des énergies marines renouvelables, les variations de bathymétrie créent de fortes fluctuations de vitesse. Il est donc essentiel de caractériser l'évolution de la turbulence provenant du fond qui pourrait impacter les chargements sur les hydroliennes. Dans ce but, des expériences sont réalisées dans un bassin à circulation en similitude de Froude avec un nombre de Reynolds aussi élevé que possible ($Fr = 0.23$ et $Re = 2.5 \times 10^5$). L'étude met l'accent sur les variations du fond à grand rapport d'aspect représentées par un cylindre à base carré de rapport d'aspect 6. L'effet de l'addition d'un cube en amont du cylindre sur le sillage est étudié. L'impact de la présence du cube sur le dévelopement du sillage est plus important que les effets de bord. Des évènements turbulents à grande échelle, produits dans le cas du cylindre, sont absents en présence du cube et aucune émission périodique de tourbillons n'est détectée.

Summary

In high flow velocity areas like those suitable for marine energy application, bathymetry variations create strong velocity fluctuations in the water column. It is therefore essential to characterize the turbulence evolution in the wake of seabed elements which may impact the loads on tidal turbines. For that purpose, experiments are carried out in a flume tank in Froude similitude with a Reynolds number as high as achievable ($Fr = 0.23$ and $Re = 2.5 \times 10^5$). The study focuses on large aspect ratio floor variations represented with a square wall-mounted cylinder of aspect ratio 6. The addition of a cube upstream of the cylinder is investigated. The cube impact on the wake development is larger than the side effects. Large scale turbulent events produced in the cylinder wake are absent with the cube and no periodic vortex shedding is detected.

I – Introduction

There is a strong tidal energy potential in France, especially in the Alderney Race [1] that presents currents up to $U_{is} = 5m/s$ (is=*in-situ*). Such areas are highly energetic for tidal turbines applications. Surveys give access to the bathymetry (figure 1) showing varied altitudes with a mean variation ($H_{is} = 5m$) leading to high Reynolds number : $R_{e,is} = H_{is}U_{is}/\nu = 2.5 \times 10^7$ and Froude number $F_{r,is} = U_{is}/\sqrt{gD_{is}} = 0.25$ ($D_{is} = 30m$ the mean depth). Such bathymetry variations are causing velocity fluctuations with a high turbulence rate in the water column. This can have a major impact on marine tidal turbines behaviour and their structural fatigue [2, 3]. Figure 1(b) illustrates bathymetry variations profiles in the area of interest for tidal turbine application. Large floor elevation is detected (in the second profile in particular), this elevation will be experimentally represented by a unitary wall-mounted obstacle. In other bathymetry elevation cases, obstacles are preceded by another obstacle of similar height. That case will be represented experimentally with a combination of two obstacles with different aspect ratios.

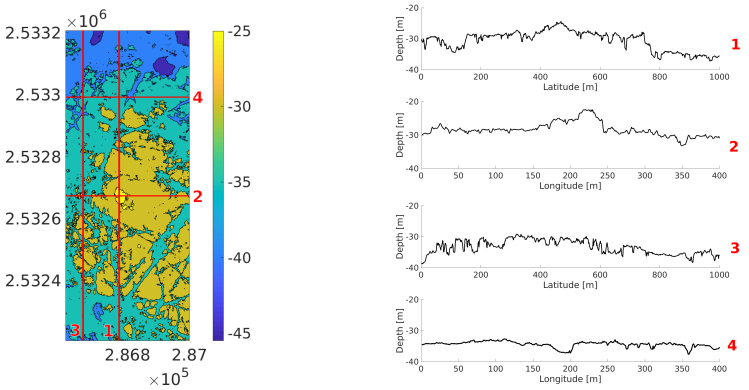

(a) Depth (m) in a $400 \times 1000m$ area of interest

(b) Bottom elevation profiles

FIGURE 1: Bathymetry of the Alderney Race (Raz-Blanchard) [4]

The flow past wall-mounted obstacles with different aspect ratios (cube, cylinder) is widely studied in the literature and a bibliographic review was already performed in previous studies [5, 6]. The combination of two or three identical wall-mounted elements is studied for example in Martinuzzi & Havel [7] or Paik *et al.* [8] for cubes and Sakamoto & Haniu [9] for cylinders. In [7], they experimentally studied the impact of the spacing of two cubes on the wake at $R_e = 2.2 \times 10^4$ and showed a shift in the wake behaviour when the spacing exceed two cube heights. However, the combination of small amount of obstacles of various aspect ratios is rare in the literature although it is closer to *in-situ* cases. The question of upstream perturbations on the wake of an obstacle has been investigated before through turbulence intensity, waves or boundary layers. No example of upstream perturbations induced by a close low aspect ratio obstacle was found.
After presenting the experimental set-up, a spatial characterization of the wake past wide wall-mounted square obstacles is presented. The effect of the addition of an upstream wall-mounted cube on the wake development is then detailed in and out of the symmetry plane. Finally, a temporal analysis is lead presenting the rise of turbulent structures in the water column for both cases.

II – Experimental Set-up

Tests have been carried out in the wave and current circulating flume tank of IFREMER located in Boulogne-sur-Mer (France) presented in figure 2. The test section is $18m$ long $\times$ $4m$ wide $\times$ $2m$ deep and the incoming flow is assumed to be steady and constant. By means of a grid combined with a honeycomb (that acts as a flow straightener) placed at the inlet of the working section (see fig. 2), a low turbulent intensity of $I = 1.5\%$ is achieved. Turbulence intensity I in the incoming flow is defined as follows :

$$I = 100\sqrt{\frac{\frac{1}{3}(\overline{u'^2} + \overline{v'^2} + \overline{w'^2})}{\overline{U_\infty}^2 + \overline{V_\infty}^2 + \overline{W_\infty}^2}} \tag{1}$$

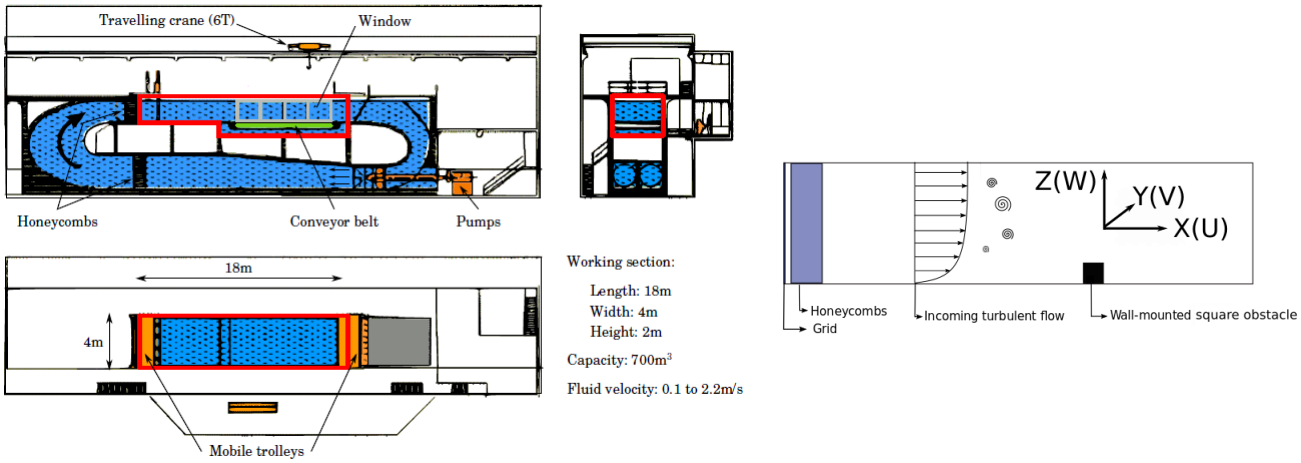

FIGURE 2: IFREMER flume tank (left) and schematic view of an obstacle in the tank (right)

In the following, average Reynolds shear stress is defined as $\tau_{uw} = \sqrt{\overline{u'w'}}$. The three instantaneous velocity components are denoted (U, V, W) along the (X, Y, Z) directions respectively (fig. 2). Each instantaneous velocity component is separated into a mean value and a fluctuation part, according to the Reynolds decomposition : $U = \overline{U} + u'$, where an overbar indicates the time average. In the following study, non dimensional lengths are used for all parameters indexed by * : $x^* = x/H$ for instance, with H the obstacle height. At the upstream obstacle position, the boundary layer height δ^* is calculated as $\delta^*_{95} = z^*(\overline{U} = 0.95\overline{U}_\infty)$. It yields $\delta^* = 1.3$. In order to consider turbulent event interaction with the free surface, experiments are achieved in Froude similitude (see table 1). Furthermore, Reynolds number must be as high as achievable to be closer to real conditions.

	Scale	U_∞ [m/s]	Rugosity height H [m]	Depth D [m]	$R_e = \frac{HU_\infty}{\nu}$	$F_r = \frac{U_\infty}{\sqrt{gD}}$
Alderney Race	1	5	5	40	2.5×10^7	0,25
Flume tank	1/20	1	0,25	2	2.5×10^5	0,23

TABLE 1: *in situ* and experimental conditions

In this study, two test cases are considered : first, a wall-mounted cylinder of dimensions : $H \times 6H \times H$, hence its aspect ratio is A_R =Width/Length=6. The cylinder represents an obstacle significantly higher than its neighbours, hence it is preceded by only the natural boundary layer developing in the tank. Second, a combination of wall-mounted obstacles is considered : a cube followed by a cylinder. The cube height is H and the cylinder has the same dimensions as above. Nomenclature is chosen as follows : C_n indicates a wall-mounted square obstacle (*i.e.* a cube or a cylinder), n is the aspect ratio. $C_n dC_m$ is a combination of obstacles where d is the spacing between consecutive obstacles, when $d = 0$, nothing is indicated. d is expressed in H units. Hence, C_6 refers to the cylinder case and $C_1 2C_6$, the cube with the cylinder case.

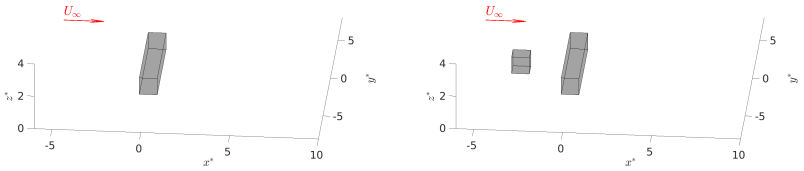

FIGURE 3: Obstacles schematic representation : C_6 (left) and $C_1 2C_6$ (right).

Two Laser Velocimetry techniques are used : LDV (Laser Doppler Velocimetry) and PIV (Particle Image Velocimetry). Beforehand, the tank is seeded with 10 μm diameter silver coated glass particles. It is synchronized with a Camera FLOWSENS EO-2M 1600 $\times$ 1200pix^2 that makes double images with a time step of 1600 μs. PIV acquisitions are made for 150s, hence 2250 double images are taken with a 15H_z acquisition frequency. The data are post processed with DYNAMIC STUDIO. Particles displacement is calculated using a Cross-Correlation [10]. Outliers are replaced with the Universal Outlier Detection [11], example and precisions on that method can be found in [12]. Positions of PIV planes are illustrated in figure 4(a) for case $C_1 2C_6$, same planes are performed for case C_6. PIV measurements are carried out at various transverse positions : $y^* = 0$, $y^* = 1$ and $y^* = 2$ (denoted $y0$, $y1$ and $y2$ respectively) represented in figure 4(b). In all positions, the measurement field is 1600 $\times$ 600 pix^2 and spatial discretizations are 11.6 mm, 12.6 mm and 13.7 mm in $y0$, $y1$ and $y2$ respectively.

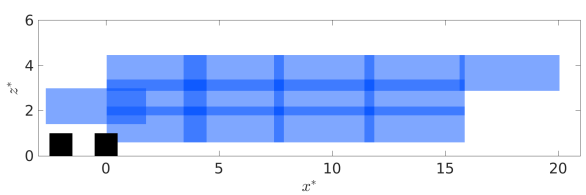

(a) PIV measurement plane for case $C_1 2C_6$

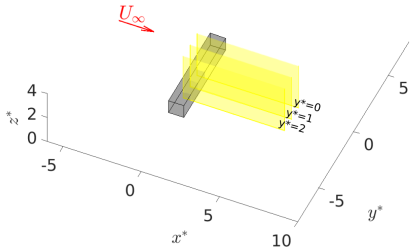

(b) Transverse position of the PIV measurement : $y0$, $y1$ and $y2$.

FIGURE 4: PIV measurement planes locations.

The LDV measurements are made using a 2D DANTEC FiberFLOW system. With LDV measurements, the acquisition frequencies are not constant. They depend on when the particles are passing through the measurement volume. Based on previous works performed in the tank [13], a re-sampling is done using the mean sample rate of the set of measurements considered. At a specific streamwise position, f_e varies from 70 to 270 H_z in the water column depending on the turbulent agitation. For the two measurement techniques, uncertainty is estimated to be around 2% for LDV and 2.6% for PIV, calculus are detailed in [12].

III – Spatial analysis

III – 1 Wall-mounted cylinder wake

An extensive study of the wake past the wall-mounted cylinder is proposed in previous study [12] and a quick review of the findings is proposed in this section. The wake past the wall-mounted cylinder is illustrated through the average streamwise velocity (fig.5) and the average Reynolds shear stress maps (fig.6). The main elements of the flow passing over a wall-mounted cubic elements can be observed : at the leading edge of the cylinder, the wake separates into the outer steady flow and the recirculation region (in blue in fig.5 : $\overline{U} < 0$). A shear layer develops in-between (fig.6) and then the flow reattaches. Recirculation length l^* is defined as the distance between the middle of the most downstream obstacle and the location where the flow reattaches downstream. l^* is evaluated at the three spanwise measurement positions : $l^*_{y0} = 6$, $l^*_{y1} = 5.4$ and $l^*_{y2} = 4.5$. When getting closer to the cylinder sides, 3D effects appear. The l^* reduction between $y0$ and $y1$ is 7% and l^* reduction increases to 21% between $y1$ and $y2$. In [14], at a similar R_e and A_R, a recirculation length of $l^* = 5.7$ has been measured in $y0$, which is close to our results. It is assumed that 3D effects do not have much impact for $|y| < y1$. Hence, the fluid presents a 2D development of the flow for $y^* \in]-1; 1[$.

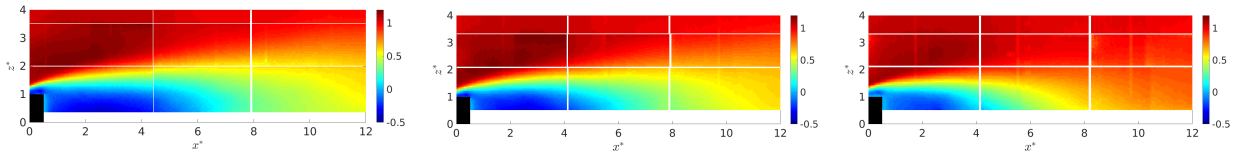

FIGURE 5: $\overline{U}$ maps for case C_6 in $y0$, $y1$ and $y2$ (left to right).

Average Reynolds shear stress τ_{uw} maps are plotted in figure 6. Some areas suffer from the poor lightning and data in these area are not fully converged. The shear layer extends beyond the measurement limits and is directed towards the free surface. It reduces faster for $y1$ compared to $y0$ although the global orientation is similar. In $y2$, the shear layer reduces by half and is reoriented towards the floor. Indeed, in $x^* = 7$, the shear layer starts disappearing for $y2$ but persists for the other two transverse positions.

III – 2 Addition of a cube upstream of the cylinder

A combination composed with a wall-mounted cylinder preceded by a wall-mounted cube is considered. Maps of $\overline{U}$ are presented in figure 7 for all transverse positions. In the symmetry plane, $l^*1.8$, which is closer to the recirculation past a cube ($l^* = 1.9$) [6] than

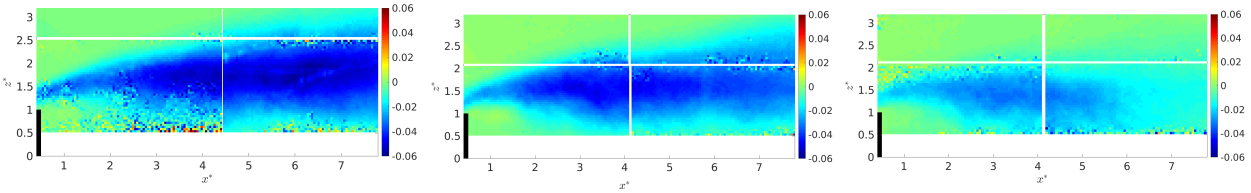

FIGURE 6: τ_{uw} maps for case C_6 in $y0$, $y1$ and $y2$ (left to right).

past a cylinder ($l^* = 6$). The recirculation bubble is very limited illustrated by a strong $\overline{U} > 0$ tendency in most of the wake. In $y1$, the recirculation region extends although its shape shows that it is still disturbed due to the cube influence. In $y2$, the wake aspect downstream of the cylinder is similar to the wake past an obstacle of aspect ratio between 1 and 6 [14]. Recirculation lengths are evaluated out of the symmetry plane : $l^*_{y1} = 4.6$ and $l^*_{y2} = 4.1$. Away from $y^* = 0$ the recirculation lengths extend although values are still lower than for the case C_6 at the same position ($l^*_{y2}(C_12C_6) < l^*_{y2}(C_6)$) indicating that the cube still has an influence at $y2$.

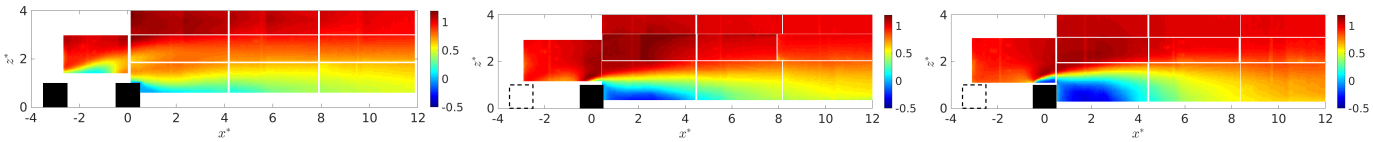

FIGURE 7: $\overline{U}$ maps for case C_12C_6 in $y0$, $y1$ and $y2$ (left to right).

In figure 8, the maps of vertical average velocity $\overline{W}$ are represented. In the symmetry plane, there is a strong $\overline{W} > 0$ area (in red in the figure) going up to $\overline{W}/U_\infty \sim 0.06$ above the cube and the cylinder. It shows that the flow is impulsed by the cube when passing over the cylinder. That area is less intense for $y1$ (up to $\overline{W}/U_\infty \sim 0.04$). It becomes intense again at $y2$ going up to $\overline{W}/U_\infty \sim 0.06$ illustrating the apparition of side effects. Downstream of the cylinder, a $\overline{W} < 0$ area (in blue) indicates the flow redirected towards the floor, that area is less and less intense when approaching the sides. This is the opposite for case C_6 [12]. Indeed, the cube presence prevents the cylinder wake from developing and from growing towards the surface. For case C_6, side effects were the most impacting on the wake evolution in the transverse direction. For C_12C_6, the most impacting factor on the wake evolution appears to be the cube presence up until $y2$.

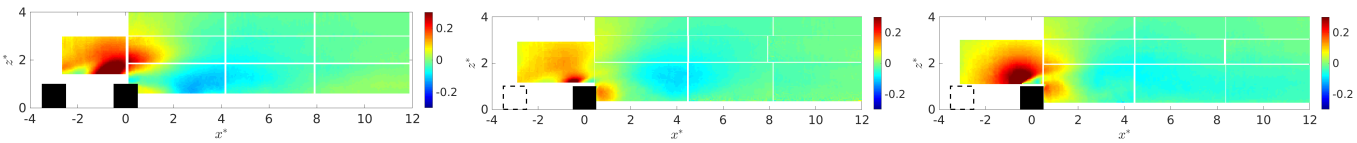

FIGURE 8: $\overline{W}$ maps for case C_12C_6 in $y0$, $y1$ and $y2$ (left to right).

The averaged Reynolds shear stress maps are presented in figure 9. In $y0$, they show a strong shear behind the cube that goes over the cylinder. Comparing to the cube alone case [6], the shear layer developing behind the cube is impulsed by the cylinder and reaches higher altitude. Values of $\tau_{uw}/U^2_\infty < -0.05$ reach a maximal altitude of $z^* = 1.5$ in the C_1 case and $z^* = 2.7$ in the C_12C_6 case. Out of the symmetry plane, the shear layer is

similar to the classic wake developing past an isolated wall-mounted obstacle. However, the shear layer reaches $z^* = 2$ in $y2$ and not in $y1$. It is prevented to go upwards in $y1$ due to the cube influence. Hence, the cylinder presence promotes the cube wake extension, as opposed to the cube presence that reduces the cylinder wake.

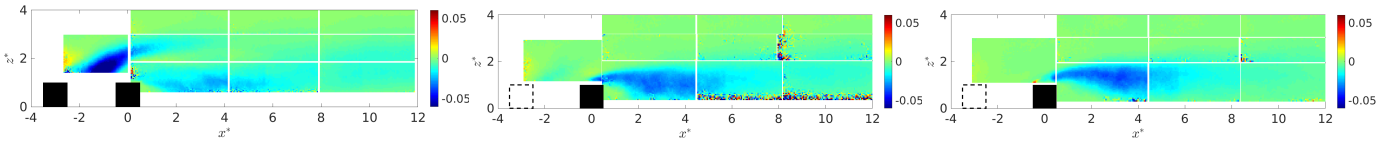

FIGURE 9: τ_{uw} maps for case $C_1 2C_6$ in $y0$, $y1$ and $y2$ (left to right).

IV – Temporal analysis

IV – 1 Instantaneous velocity fields

Using PIV measurements, cases C_6 and $C_1 2C_6$ are compared in terms of fluctuating velocities. In figure 10, $u'w'$ is plotted on a z^* versus t maps at $x^* = 13.5$ for the $150s$ of the acquisition. A vortex passing is indicated with a $u'w' > 0.03$ followed by a $u'w' < -0.03$. For case $C_1 2C_6$, in figure 10(b), less than 10 vortices are detected and only two of them reach the highest altitude (both vortices are around $t \sim 110s$). However, for case C_6 in figure 10(a), at mid-height ($z^* = 3.5$), periodic vortex passing is observed. Furthermore, most of the vortices have an impact on the flow until the highest altitude. Results out of the symmetry plane for $C_1 2C_6$ show that the number of vortices detected in $y1$ is as low (< 10) as in $y0$ and only one turbulent event reaches the highest altitude. In $y2$, although the shear layer reaches higher altitude (as explained earlier in fig.9), no vortex intense enough to be detected (using a vortex detection algorithm developed in [12]) passes through the measurement plane. Despite the reduction of the cube influence in $y2$, no vortex are energetic enough to reach $z^* = 3.1$ at the selected streamwise position.

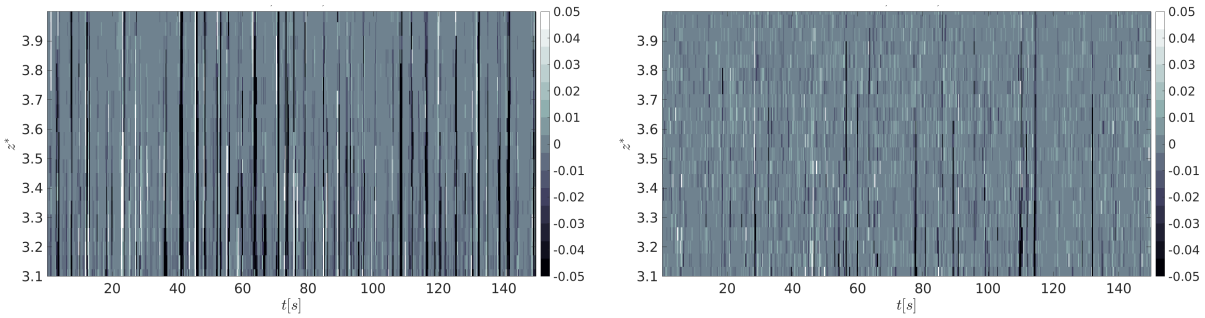

(a) (b)

FIGURE 10: $u'w'$ in a z^* versus t map in $y0$ at $x^* = 13.5$, from PIV measurements for test cases C_6 (left) and $C_1 2C_6$ (right).

At $x^* = 13.5$ and in the symmetry plane, two altitudes are selected : $z^* = 3.2$ and $z^* = 4$. $u'w'$ signals are represented in figure 11. Test case C_6 induces larger fluctuations that persist higher in the water column. Case $C_1 2C_6$ shows only few energetic events at

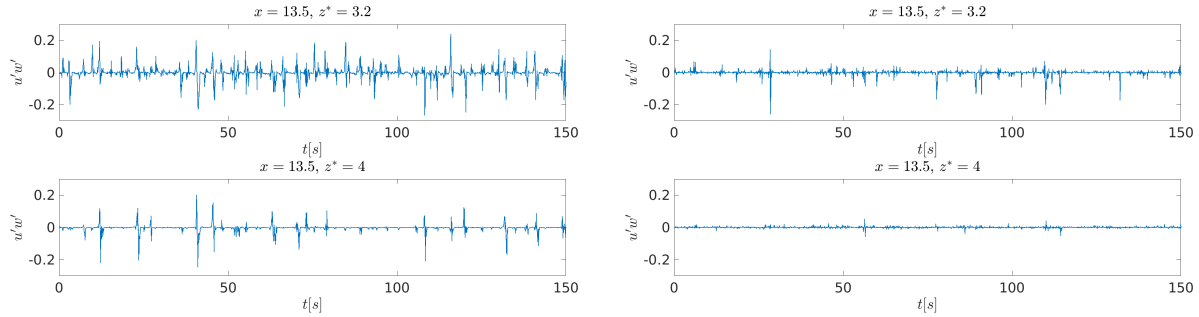

(a) (b)

FIGURE 11: $u'w'$ signals from PIV measurements in $y0$ at $x^* = 13.5$ and for altitudes $z^* = 3.2$ (top) and $z^* = 4$ (bottom). Test cases C_6 (left) and C_12C_6 (right).

the lowest altitude and almost nothing in comparison at the highest altitude.

In figure 11, the most energetic events are identified : at $t \sim 40s$ for C_6 and $t \sim 28s$ for C_12C_6. Their fluctuating velocity fields are represented in figure 12. The vortex generated in the C_6 wake is larger and more energetic than the one created in the C_12C_6 wake. Due to the cube presence, the vortex organisation that develops in the wake of the cylinder is shattered. The cube presence induces a wake that disturbs the vortex organisation developing downstream of the cylinder : no large coherent structures as the one observed in figure 12(a) can be generated with the cube presence.

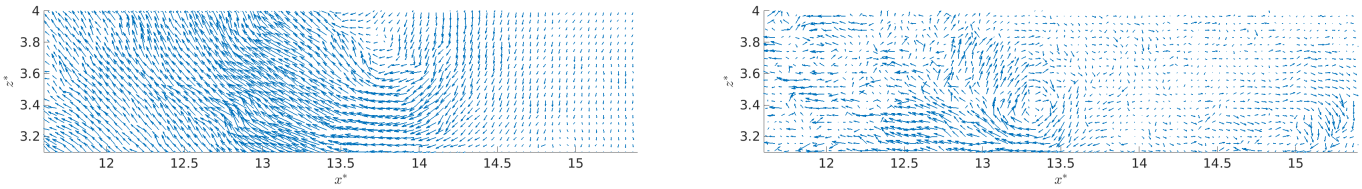

(a) Case C_6, $t = 40.8s$ (b) Case C_12C_6, $t = 28.3s$

FIGURE 12: Instantaneous fluctuating velocity field for test cases C_6 (left) and C_12C_6 (right).

IV – 2 Shedding frequency

Using LDV measurements, a temporal analysis is lead. More details on the LDV post-processing method can be found in previous works [12]. After a re-sampling of the LDV signals, a Fast Fourier Transform is applied and Power Spectrum Densities (PSD) are plotted versus the Strouhal number $S_t = fH/U_\infty$. Results for the streamwise velocity fluctuations for both cases are presented in figure 13(a) in the symmetry plane. A sharp peak is detected for C_6 at both altitudes at $S_t = 0.07$. It is close to the results found in the literature for dune cases [15] and consistent with the periodic shedding of vortices from the wake. The frequency detected here matches the periodic passing on vortices in figure 10. In [16], it is explained that the peak is detected on the u' and w' components only due to the absence of side effects in the symmetry plane. For case C_12C_6, the amplitude is similar to C_6 for higher frequencies, indicating a similar turbulent energetic level at a given position. However, no peak is detected on the spectra. As explained before, in the wake of C_12C_6,

the turbulent flow is not coherent enough to generate periodically shed structures. In order to evaluate the obstacle impact on the water column, average streamwise velocity profiles are represented in figure 13(b) for both cases at various streamwise positions and for the available data. In the first two positions ($x^* = 1$ and $x^* = 3$), mean flow variations of C_12C_6 reach higher altitude. As developed before, the cube presence impulses the cylinder wake higher in the water column. However, at the furthest positions, the C_6 wake shows a velocity deficit up to highest positions represented ($z^* = 4$) whereas C_12C_6 profiles show that the outer flow is restored above $z^* \sim 3$. Indeed, as developed before, C_6 wake is impulsed towards the surface whereas C_12C_6 wake is not.

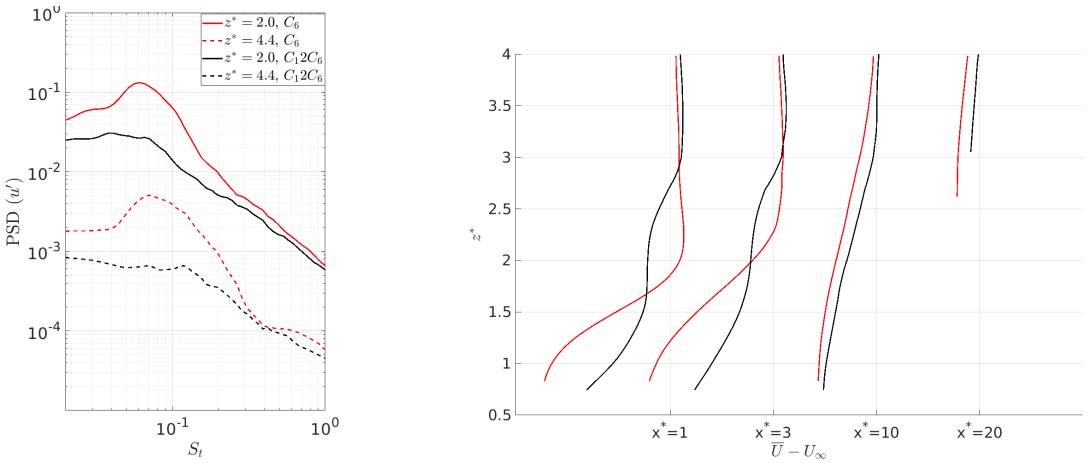

(a) PSD spectrum of u' in $x^* = 11$ for $z^* = 2.0$ $(-)$ and $z^* = 4.4$ $(--)$.

(b) $\overline{U}$ velocity profiles at $x^* = 1$, $x^* = 3$, $x^* = 10$ and $x^* = 20$.

FIGURE 13: Evaluation of the C_6 (red) and C_12C_6 (black) wake extension through temporal (left) and spatial (right) analysis.

V – Conclusion & Perspectives

The wake past obstacles representative of seabed elements is investigated. Measurements are carried out in a flume tank in Froude similitude and at high Reynolds number. First, the case of an isolated wall-mounted cylinder is investigated, it has been studied in previous studies and a summary is proposed here. In the symmetry plane, due to the absence of side effects, the wake extends, the recirculation length is $l^*_{y0} = 6$. When getting closer to the obstacle ends ($y1$ and $y2$), side effects redirect the wake towards the floor and the wake reduces. In most of the bathymetry, obstacles are to be considered in combination. Hence, a cube is added upstream of the cylinder. Its presence strongly impacts the cylinder wake and, in the symmetry plane, the recirculation length is 3 times inferior to the cylinder case. Closer to the ends ($y1$ and $y2$), the cube presence influence reduces and the wake extends. The cube has a greater impact on the cylinder wake development compared to the side effects. Velocity maps also illustrate that the cylinder presence promotes the cube wake development. Using PIV and LDV measurements, a temporal analysis is lead. Results show that the cylinder produces periodically shed turbulent structures that rise up in the water column. It is then showed that the addition of a cube breaks the structure organization of the cylinder. Indeed, turbulent structures

are almost absent, they do not rise in the water column and those observable are smaller and less energetic than those produced without the cube. Spectra show the absence of shedding peak in the case with the upstream cube. Mean velocity profiles for each case are represented : with the cube, mean flow variations rise in the water column but only close to the cylinder, without the cube, they rise much higher in the far wake of the cube ($x^* > 3$). To conclude, whether an obstacle is isolated (*i.e.* substantially higher than the average bathymetry variation around it) or preceded by another obstacle as high, the wake development is different. Turbulent events rising up in the water column are present only for the first case. These events, combined with intense average fluctuating velocities will have a strong impact on tidal turbine fatigue and production. Hence, the presence of an obstacle upstream of a large aspect ratio element must be accounted for in the design and the positioning of marine tidal turbines.

Acknowledgement

This work benefits from a French State grant managed by the National Research Agency under the Investments for the Future program bearing the reference ANR-10-IEED-0006-11. The authors also acknowledge the financial support of Ifremer and the Hauts de France Regional Council for this PhD study. We are grateful to the French navy SHOM ("Service Hydrographique et Océanographique de la Marine") for providing access to bathymetric data (http ://data.shom.fr/). We are most grateful to Thomas Bacchetti, Inès Belarbi and Jean-Valery Facq for their assistance and precious advices.

Références

[1] L. Myers and A. Bahaj, "Simulated electrical power potential harnessed by marine current turbine arrays in the alderney race," *Renew. Energ.*, vol. 30, pp. 1713–1731, 2005.

[2] O. Duràn Medina, F. Schmitt, R. Calif, G. Germain, and B. Gaurier, "Turbulence analysis and multiscale correlations between synchronized flow velocity and marine turbine power production," *Renew. Energ.*, vol. 112, pp. 314–327, 2017.

[3] P. Mycek, B. Gaurier, G. Germain, G. Pinon, and E. Rivolaen, "Experimental study of the turbulence intensity effects on marine current turbines behaviour. part I : One single turbine," *Renew. Energ.*, vol. 66, pp. 729–746, 2014.

[4] SHOM, "MNT bathymétrique de façade atlantique (projet homonim)." 2015.

[5] M. Ikhennicheu, P. Druault, B. Gaurier, and G. Germain, "An experimental study of influence of bathymetry on turbulence at a tidal stream site," *EWTEC, Cork, Ireland*, 2017.

[6] M. Ikhennicheu, B. Gaurier, P. Druault, and G. Germain, "Experimental analysis of the floor inclination effect on the turbulent wake developing behind a wall mounted cube," *Eur. J. Mech. B/ Fluid*, vol. 72, pp. 340–352, 2018.

[7] J. Martinuzzi and B. Havel, "Vortex shedding from two surface-mounted cubes in tandem," *Int. J. Heat Fluid F.*, vol. 25, pp. 364–372, 2004.

[8] J. Paik, F. Sotiropoulos, and F. Porté-Agel, "Detached eddy simulation of flow around two wall-mounted cubes in tandem," *Int. J. Heat Fluid Fl.*, vol. 30, pp. 286–305, 2009.

[9] H. Sakamoto and H. Haniu, "Effect of free-stream turbulence on characteristics of fluctuating forces acting on two square prisms in tandem arrangement," *J. Fluid Eng.*, vol. 110, pp. 140–146, 1988.

[10] C. Meinhart, A. Prasad, and R. Adrian, "A parallel digital processor system for particle image velocimetry," *Meas. Sci. Technol.*, vol. 4, pp. 619–626, 1993.

[11] J. Westerweel and F. Scarano, "Universal outlier detection for PIV data," *Exp. Fluids*, vol. 39, pp. 1096–1100, 2005.

[12] M. Ikhennicheu, G. Germain, P. Druault, and B. Gaurier, "Experimental study of coherent flow structures past a wall-mounted sqaure cylinder," *Under review in Exp. Fluids*.

[13] O. Duràn Medina, F. Schmitt, R. Calif, G. Germain, and B. Gaurier, "Correlation between synchronised power and flow measurements, a way to characterize turbulent effects on a marine current turbine," *EWTEC*, 2015.

[14] R. Martinuzzi and C. Tropea, "The flow around surface-mounted, prismatic obstacles placed in a fully developed channel flow, *(Data Bank Contribution)*," *J. Fluid Eng.*, vol. 115, pp. 85–92, 1993.

[15] M. Omidyeganeh and U. Piomelli, "Large-eddy simulation of two-dimensional dunes in a steady, unidirectional flow." *J. Turbul.*, vol. 42, pp. 1–31, 2011.

[16] M. Ikhennicheu, G. Germain, B. Gaurier, and P. Druault, "Experimental study of the wake past cubic wall-mounted elements to predict flow variations for tidal turbines," *AWTEC, Taipei, Taiwan*, 2018.